Int6 Expression Can Predict Survival in Early-Stage Non–Small Cell Lung Cancer Patients

Fiamma Buttitta,[1] Carla Martella,[1] Fabio Barassi,[1] Lara Felicioni,[1] Simona Salvatore,[1] Sandra Rosini,[1] Tommaso D'Antuono,[1] Antonio Chella,[2] Felice Mucilli,[3] Rocco Sacco,[3] Andrea Mezzetti,[1] Franco Cuccurullo,[1] Robert Callahan,[4] and Antonio Marchetti[1]

Abstract

Purpose: The *Int6* gene was originally identified as a common insertion site for the mouse mammary tumor virus in virally induced mouse mammary tumors. Recent studies indicate that Int6 is a multifaceted protein involved in the regulation of protein translation and degradation through binding with three complexes: the eukaryotic translation initiation factor 3, the proteasome regulatory lid, and the constitutive photomorphogenesis 9 signalosome. This study aimed to investigate the prognostic role of Int6 in a large series of stage I non–small cell lung cancers (NSCLC) patients with long-term follow-up.

Experimental Design: We determined the methylation status of *Int6* DNA by methylation-specific PCR and the steady-state levels of *Int6* RNA by quantitative real-time reverse transcription-PCR in 101 NSCLCs and matched normal lung tissues.

Results: In 27% of the tumors, *Int6* RNA levels were reduced relative to normal tissue. In 85% of the tumors with reduced *Int6* expression, the transcription promoter and first exon were hypermethylated, whereas only 4% of the tumors with elevated *Int6* RNA levels were hypermethylated ($P < 0.000001$). Low levels of *Int6* RNA were found a significant predictor of overall and disease-free survival ($P = 0.0004$ and $P = 0.0020$, respectively). A multivariate analysis confirmed that low *Int6* expression was the only independent factor to predict poor prognosis, for both overall ($P = 0.0006$) and disease-free ($P = 0.024$) survival.

Conclusions: Our results suggest that *Int6* expression, evaluated by quantitative real-time PCR, may represent a new prognostic factor in patients with stage I NSCLC.

The *Int6* gene was first identified as a common insertion site for mouse mammary tumor virus in virally induced mouse mammary tumors and a preneoplastic lesion (1). In each case, mouse mammary tumor virus integrated into an intron in the opposite transcriptional orientation of *Int6*. Transcription of the affected allele was terminated at a cryptic transcription stop signal in the reverse mouse mammary tumor virus long terminal repeat sequence causing the expression of a truncated chimeric RNA that encodes a COOH-terminally deleted product. Overexpression of these truncated proteins can confer the capability of anchorage-independent growth on mammary epithelial cells and fibroblasts in culture and injection of these cells into nude mice can lead to tumor development (2, 3). Because we found no mutations in the remaining allele of the mouse mammary tumor virus–induced tumors, we have hypothesized that the truncated Int6 protein may act as dominant-negative oncoprotein.

The *Int6* gene has been highly conserved through evolution, from fission yeast to humans, with the intriguing exception of budding yeasts that have a related protein called Pci8p (4). Int6 was later independently rediscovered several times by investigators working in different areas of biological research (5). Asano et al. found that Int6 is identical to the p48 subunit of the eukaryotic translation initiation factor3 (eIF3) complex that plays a pivotal role in the initiation phase of protein synthesis by promoting the binding of both methionyl-tRNA and mRNA to the 40S ribosomal subunit (6). However, Int6 is not essential for translation initiation in fission yeast. Moreover, the eIF3 complex is unstable in the absence of Int6 (7, 8). These and other observations suggest that Int6 is a regulatory subunit of the eIF3 complex. Other studies conducted on the fission yeast *Saccharomyces pombe* have shown that yin6, the yeast Int6 homologue, positively regulates the 26S proteasome by binding to and mediating the nuclear import and assembly of a proteasome regulatory subunit, Rpn5 (9). Indeed, Int6 seems a multifaceted protein in that through its proteasome/constitutive photomorphogenesis 9 signalosome/eIF3 domain, it can bind not only the eIF3

Authors' Affiliations: [1]Clinical Research Center, Center of Excellence on Aging, University Foundation, Chieti, Italy; [2]Department of Surgery, University of Pisa, Pisa, Italy; [3]Department of Surgery, University of Chieti, Chieti, Italy; and [4]Oncogenetic Section, Mammary Biology and Tumorigenesis Laboratory, National Cancer Institute, NIH, Bethesda, Maryland

Received 11/10/04; revised 1/25/05; accepted 2/9/05.

Grant support: Centro Nazionale Ricerche/Ministero dell'Università e della Ricerca Scientifica e Tecnologica, Center of Excellence on Aging, and Fondo per gli Investimenti della Ricerca di Base.

The costs of publication of this article were defrayed in part by the payment of page charges. This article must therefore be hereby marked *advertisement* in accordance with 18 U.S.C. Section 1734 solely to indicate this fact.

Requests for reprints: Antonio Marchetti, Pathology Unit, Clinical Research Center, Center of Excellence on Aging, University Foundation, Via Colle Dell'Ara, 66013 Chieti, Italy. Phone: 39-871-357407, ext. 408; Fax: 39-871-540079; E-mail: amarchetti@unich.it.

and the proteasome regulatory lid but also the constitutive photomorphogenesis 9 signalosome, which is best known for its role in plants to regulate photomorphogenesis (10–12). The constitutive photomorphogenesis 9 signalosome is predominantly nuclear (10), eIF3 is cytoplasmic, and the proteasome can be distributed in both cell compartments (11, 12). Because Int6 contains a bipartite nuclear localization sequence and a putative NH_2-terminal nuclear export signal (13), it can shuttle between the nucleus and the cytoplasm and interact with these three complexes (14). All of these observations suggest that Int6 could exert a regulatory activity in both protein translation and degradation and possibly act on specific transcripts (15).

Int6 is located on human chromosome 8q22-q23 (16). To determine whether it is a target for mutation during human tumor development, Miyazaki et al. (16) surveyed 100 primary breast tumor DNAs. They found loss of heterozygosity (LOH) in 11 of 39 (28%) of primary breast carcinoma DNAs that were informative for a polymorphic sequence in *Int6* intron 7. However, because single-strand conformation and hybrid mismatch analysis of the remaining allele in these tumor DNAs failed to detect any mutations, they concluded that the target gene for LOH was not *Int6* but a gene closely linked to *Int6*. In another study, we observed a reduction of *Int6* expression in 37% of 62 breast carcinomas and 31% of 78 non–small cell lung carcinomas (NSCLC; ref. 17). No significant association was found between *Int6* expression and LOH status suggesting that LOH is not involved in the down-regulation of the gene. In the present study, we have examined an independent large series of stage I NSCLC with long-term follow-up for *Int6* expression by quantitative real-time reverse transcription-PCR (RT-PCR) and the methylation status of the *Int6* transcription promoter and first exon. Our results show that in approximately one fourth of these cases, regulatory regions within the *Int6* gene are methylated, *Int6 RNA* levels are low, and the tumors are more aggressive with the patients having a reduced overall survival and decreased disease-free survival.

Materials and Methods

Patients and tissues. The tumors for this study were obtained from a consecutive series of 112 stage I (T1-2 N0 M0) NSCLC patients surgically treated at the Department of Surgery, University of Pisa (Pisa, Italy) between 1993 and 1994. The study was conducted on 101 of these patients for which tissues and complete follow-up data were available. Informed consent was obtained from all patients under study. In each case, tumor and macroscopically normal lung tissue samples (taken as far as possible from the neoplastic area) were snap-frozen in liquid nitrogen within 10 minutes of excision and stored at −80°C. Pieces of tumor and normal tissues, immediately adjacent to the corresponding frozen samples, were fixed and processed for light microscopy. In all tumor specimens, the amount of tumor cells equaled or exceeded 80% of the overall sample, confirmed by histopathologic examination. Similarly, all the macroscopically normal samples were judged to be histologically normal. The study population consisted of 93 men (92%) and 8 women (8%), with a mean age of 62.8 years (range, 43-74 years). Patients underwent lobectomy (83% of cases) or pneumonectomy (17% of cases) with hylar and mediastinal lymph nodes sampling. Patient stage at the time of diagnosis was determined according to the guidelines of the American Joint Committee on Cancer (18). Based on sizes, 32 (32%) tumors were classified as T1 and 69 (68%) tumors as T2. Histologic type and tumor cell differentiation were determined according to the WHO criteria (19). The most common histologic type was squamous cell carcinoma (55 cases, 54%), followed by adenocarcinoma (32 cases, 32%), bronchioloalveolar carcinoma (10 cases, 10%), and large cell carcinoma (4 cases, 4%). Twenty-eight (28%) tumors were well differentiated (G1), 40 (40%) moderately differentiated (G2), and 33 (33%) poorly differentiated (G3). Smoking history was available for 88 patients: 53 (60%) were smokers, 32 (37%) were former smokers (stopped smoking at least 1 year before the diagnosis of lung cancer), and 3 (3%) were nonsmoker.

Follow-up data of the study population were obtained by direct patient contact. Follow-up occurred at 2-month intervals for the initial 2 years and at 4-month intervals afterward. Recurrences were detected by computed tomography scans or scintigrams and confirmed by pathologic examination, using biopsies specimens. Patients were categorized as alive with evidence of disease, alive without disease, and dead as a result of lung carcinoma. No patient in this series died of cancer-unrelated causes. Time in days from the date of the operation to the date of follow-up or death was recorded. The median follow-up in the series of patients examined was 55 months (range, 7-94 months).

RNA extraction and cDNA synthesis. Total RNA was extracted from frozen tumor and normal tissue specimens by using a commercial kit, TRIzol (Life Technologies, Carlsbad, CA), according to the manufacturer's protocol. RNA was quantified spectrophotometrically, and its quality was checked by electrophoresis through agarose gels stained with ethidium bromide. Total RNA (200 ng) was reverse transcribed in a total volume of 50 μL containing 1× buffer, 5.5 mmol/L $MgCl_2$, 1 mmol/L deoxynucleotides, 2.5 μmol/L random hexamers, 20 units RNase inhibitor, and 62.5 units MuLv reverse transcriptase. The samples were incubated at 25°C for 10 minutes, 48°C for 30 minutes, and 95°C for 5 minutes.

PCR amplification. PCR was done in a total volume of 50 μL containing 1× Taqman buffer; 5.5 mmol/L $MgCl_2$; 200 μmol/L dATP, dCTP, dGTP, and 400 μmol/L dUTP; 300 nmol/L each primer; 100 nmol/L probe; 0.5 unit of AmpErase UNG; 1.25 units AmpliTaq Gold; and 10 μL of cDNA. β-Actin, β2-microglobulin, and *Int6* amplification were done in duplicate for each sample. The thermal cycling conditions included 2 minutes at 50°C and 10 minutes at 95°C followed by 40 cycles of 95°C for 15 seconds and 60°C for 1 minute. All reagents used for RT-PCR were purchased from Applied Biosystems (Foster City, CA).

Primers and probes. Because the human *Int6* gene has three processed pseudogenes that are located on chromosomes 2, 6, and 13 (Genbank accession nos. NG_001023.1, AC107075.4, and AL354696.11, respectively), we designed a pair of oligonucleotide primers that specifically amplify a 141-bp fragment of the human *Int6* reverse-transcribed mRNA but not the related pseudogene sequences. The primer probe set for *Int6* was forward primer 5′-GACACATTGTCTGAATTGCATTAAGAT-3′, reverse primer 5′-CACTTCAGTCTCTTCAGCAGAGAAC-3′, and Taqman probe (FAM)-TGATTGAAGAAAACAAACAGAGACCAGTGAATGA-(TAMRA). Primers and probe for *Int6* mRNA were generated using a dedicated computer program, Primer Express (Applied Biosystems). For amplification of β-actin and β2-microglobulin mRNAs, commercially available primers and probes (Applied Biosystems) were used.

Real-time reverse transcription-PCR analysis. *Int6* expression in tumors and matching normal lung samples was measured by real-time quantitative RT-PCR, based on Taqman methodology, using the ABI PRISM 7900 Sequence Detection System (Applied Biosystems). This technique allows, by means of fluorescence emission, to find the cycling point when PCR product is detectable (C_t value or threshold cycle). As previously reported, the C_t value correlates to the starting quantity of target mRNA (20). To accurately normalize the amount of total RNA present in each reaction, we amplified two housekeeping genes *β-actin* and *β2-microglobulin*, which are assumed constant in both normal samples and lung carcinomas. Our results are expressed as relative levels of *Int6* RNA referred to a sample, called calibrator, chosen to represent 1× expression of this gene. The calibrator used was a normal lung of the

tissue collection under study, arbitrarily selected, that was analyzed on every assay plate with the unknown samples. All the analyzed tumors express *n*-fold Int6 mRNA relative to the calibrator. The amount of target, normalized to endogenous references (β-actin and β2-microglobulin) and relative to the calibrator was defined by the C_t method as described by Livak K (Sequence Detector User Bulletin 2, Applied Biosystems). Specifically, the formula was applied as follows: target amount = 2^{-Ct}, where C_t = {[C_t (*Int6* sample) − mean C_t (β-actin, β20microglobulin sample)] − [Ct (*Int6* calibrator) − mean C_t (β-actin, β2-microglobulin calibrator)]}.

This method is based upon the assumption that the target (Int6) and the references (β-actin and β2-microglobulin) display equal amplification efficiencies. To verify this condition, we checked C_t [C_t Int6 − mean C_t (β-actin, β2-microglobulin)] variations according to template dilution. We prepared a standard curve, composed of five different dilutions of total RNA obtained from a lung tumor tissue (100, 25, 6.25, 1.6, and 0.4 ng). The slope of this curve was 0.063. To ensure the appropriate amplification efficiency, the slope of the standard curve should be <0.1.

DNA extraction and bisulfite treatment. DNA was extracted from tumor and matched normal specimens using standard methods. The bisulfite modification of genomic DNA was done using the Intergen CpGenome DNA modification kit (Intergen Co., Purchase, NY). In brief, 1 μg of genomic DNA was placed in 100 μL of water and denatured by adding 7.0 μL of 3 mol/L NaOH for 10 minutes at 37°C. To each denatured DNA solution, 550 μL of freshly prepared sodium bisulfite mixture (Intergen) were added and the solutions were incubated at 50°C for 16 to 20 hours. After bisulfite modification, all unmethylated cytosines (but nonmethylated cytosines) are deaminated and converted to uracils, which are then converted to thymidine during the subsequent PCR amplification, resulting in sequence differences between methylated and unmethylated DNA. The DNA samples were then purified by ethanol precipitation and resuspended in 25 to 50 μL of TE [10 mmol/L Tris and 0.1 mmol/L EDTA (pH 7.5)].

Methylation-specific PCR assay. The methylation status of *Int6* gene was determined by methylation-specific PCR as described by Herman et al. (21). PCR amplification was done with methylation-specific primers that were designed to distinguish methylated from unmethylated DNA. Primer sequences for the methylated form were forward primer 5′-TTTTGGGCGTAAGGAAGGCGT-3′ and reverse primer 5′-GCGGTCGCGAGTTTGGTTTT-3′. Primer sequences for the unmethylated form were forward primer 5′-TTGGGTGTAAGGAAGGTGTGG-3′ and reverse primer 5′-GTGAGGTGGTTGTGAGTTTGGTT-3′. Annealing temperature for the methylated form primers was 62°C and for the unmethylated form primers was 58°C. For each set of DNA modification and PCR, normal human lymphocyte DNA *in vitro* methylated with *Sss*I methylase according to the manufacturers instructions (New England Biolab, Beverly, MA) was used as a positive control, normal lymphocyte DNA was used as a negative control, and water with no DNA template was used as a control for contamination.

Statistical methods. The means of *Int6* RNA levels in normal and lung tumor samples were compared using the paired samples *t* test. The relationships between *Int6* RNA levels and clinicopathologic variables were assessed by Fisher's exact test or χ^2 test as appropriate. The survival curves were estimated using the Kaplan-Meier method, and differences among them evaluated by the log-rank test. Disease-free survival was defined as the period between surgery and the first local recurrence, the evidence of distant metastasis or the end of the study. Overall survival was defined as the period from surgery to the patient's death. Cox's proportional hazards regression model was used to assess the effect of *Int6* expression on disease-free and overall survival after adjustment for tumor size (T_1 versus T_2), histologic type (squamous carcinoma versus other histotypes), and tumor grade (G1-2 versus G3). The assumptions of the proportional hazards model were checked by plotting the log of the cumulative hazard function. $P = 0.05$ was considered significant.

Results

Int6 RNA levels in 101 NSCLCs and matching normal lung tissues were determined by quantitative real-time RT-PCR. To accurately quantify the expression of *Int6*, two housekeeping genes (*β-actin* and *β2-microglobulin*) were amplified and the mean of data in each case was used to normalize results, as detailed in the previous section. In normal lung tissues, *Int6* RNA levels ranged from 0.15 to 2.95, with a mean of 0.60, whereas in NSCLC samples *Int6* RNA levels ranged from 0.07 to 10.70, with a mean of 1.39. A paired *t* test analysis showed that the mean of *Int6* RNA levels in tumor tissues was significantly ($P = 0.000001$) higher than that observed in normal lung tissues.

The ratio of *Int6* RNA levels in primary tumor and corresponding normal lung tissue was calculated for all cases (Fig. 1). This ratio ranged from 0.076 to 15.14 with a mean of 2.94 (SE, 0.32). Setting a cutoff at a ratio of 1, we observed that 74 tumors (73.3%, Fig. 1, *solid columns*) had *Int6* RNA levels greater than that observed in matching normal lung tissues, whereas 27 tumors (26.7%, Fig. 1, *open columns*) had reduced levels of *Int6* RNA. To ascertain whether the elevated levels of *Int6* RNA in the tumors were associated with the amplification of the gene, we did real-time PCR on tumor and matching normal genomic DNA. However, in no case was there evidence of gene amplification.

Methylation of the Int6 promoter and exon 1. Nucleotide sequence analysis of the *Int6* gene revealed a CpG island located around and within the first exon, harboring 54 potential methylation sites (Fig. 2A, *vertical bars*). This region satisfied the criteria of Gardiner-Garden and Frommer, in that it was 1,110 bp long with a G + C content over 50%, and an observed/expected CpG dinucleotide ratio > 0.6 (22). To evaluate the methylation status of selected CpG sites, we developed a methylation-specific PCR assay of bisulfite-treated DNA (Fig. 2B). We found that 23 (85%) of the 27 tumors with reduced levels of *Int6* RNA had hypermethylation of the *Int6* promoter and exon 1 (compare Fig. 2B1 and B2 with B4), whereas only 3 (4%) of the 74 tumors which had high levels of Int6 RNA were hypermethylated in this region of *Int6* ($P < 0.000001$). Interestingly, hypermethylation of *Int6* was also present in 28% of normal lung tissues when the corresponding tumor was hypermethylated (Fig. 2B3). There were no cases of Int6 hypermethylation in normal lung DNA when the *Int6* sequence in the corresponding tumor was unmethylated.

Correlation with clinicopathologic variables and survival analysis. No statistically significant association was found between Int6 expression or methylation and clinicopathologic variables, such as age, sex, histologic type, tumor size, and degree of tumor differentiation or smoking habits (Table 1 and data not shown). The 5-year survival rate of the series of patients was 70%. The median time to recurrence was 22 months (range, 3-56 months); the recurrence rate was 34 of 101 (34%), and the recurrences were initially located at a distant site in 26 cases (26%) or within the ipsilateral hemithorax in eight cases (8%). Univariate overall (Fig. 3A) and disease-free (Fig. 3B) survival curves, estimated using the method of Kaplan and Meier, defined a significantly worse prognosis for patients with low *Int6* RNA levels. The 5-year overall survival rates for high-*Int6* and low-*Int6* patients were 80% and 43% ($P = 0.0004$), respectively. Int6 expression proved to affect disease-free survival as well:

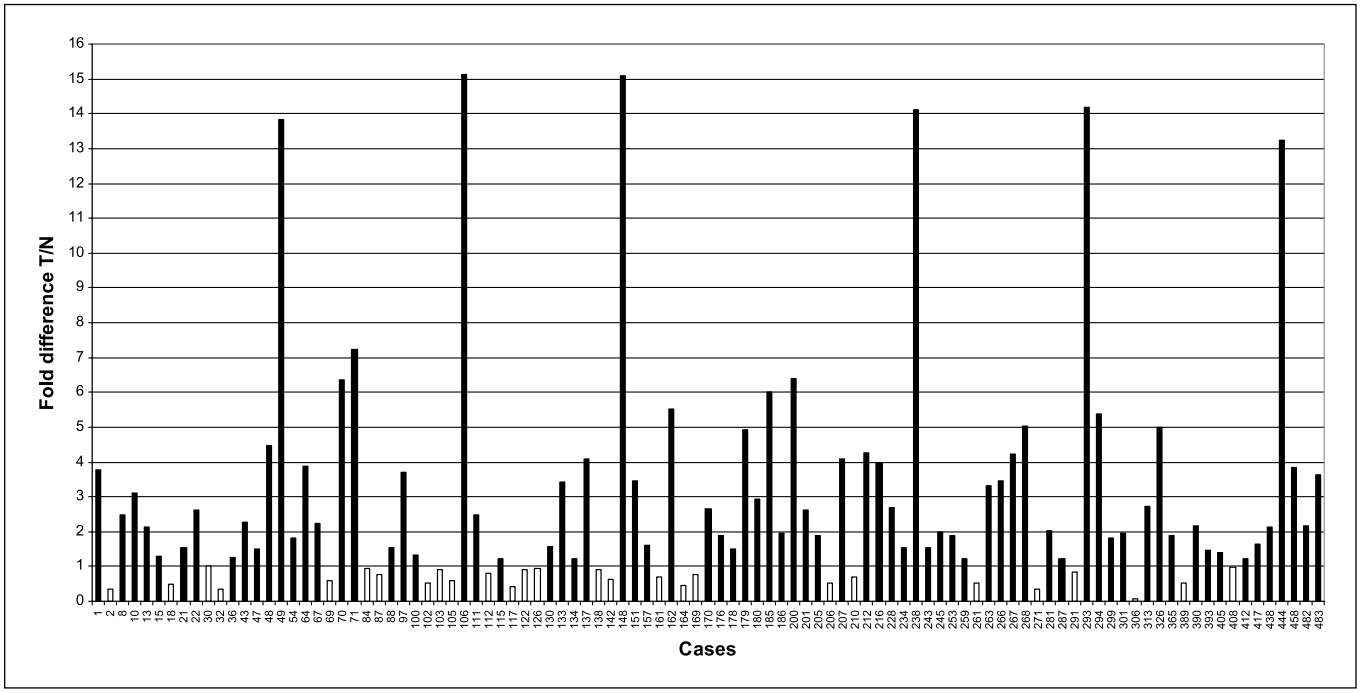

Fig. 1. Real-time quantitative RT-PCR analysis of *Int6* expression in the 101 NSCLCs and matching normal lung samples. Fold difference indicates the ratio of *Int6* levels in neoplastic and normal tissue. *Black and white columns,* tumors in which the fold difference was >1 or <1, respectively.

the 5-year survival rates were 81% for the patients with high Int6 expression and 42% for the patients with low Int6 expression ($P = 0.002$). There was no significant correlation between overall or disease-free survival and T status, histologic type, and histologic grade of the tumor. The joint effect of tumor size, histologic type, and histologic grade were examined using stepwise Cox regression. The multivariate analysis confirmed that Int6 expression was the only independent and significant factor to predict poor prognosis, for both overall ($P = 0.0006$) and disease-free ($P = 0.024$) survival (Table 2).

Discussion

In this study, we have analyzed by quantitative real-time RT-PCR the expression status of *Int6* in a large series of stage I NSCLCs with long-term follow-up. For all patients, frozen samples from primary tumors and matching normal lung tissues were available. In each case, Int6 expression was evaluated in tumor (T) and normal (N) samples and the T/N ratio was calculated. To accurately quantify the expression of Int6, two housekeeping genes were amplified and the mean of

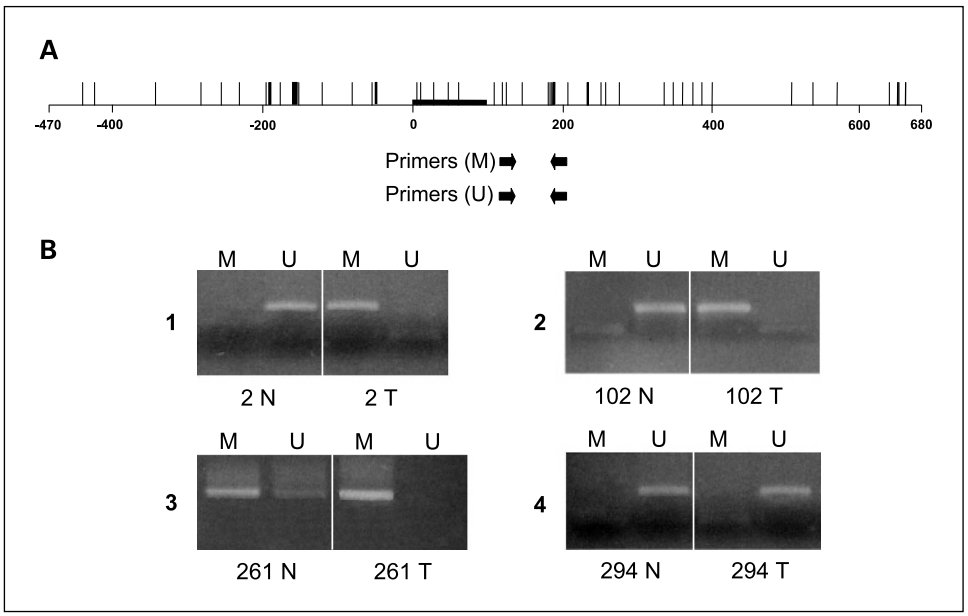

Fig. 2. *A*, schematic map of the *Int6* CpG island located around and within the exon 1 (*horizontal black bar*) of the gene; CpG density (*short vertical bars*). Arrows, PCR primers: unmethylated (*U*) and methylated (*M*). Numbering in this scheme corresponds to position relative to the transcription start site. *B*, analysis of aberrant methylation of the *Int6* gene in tumor (*T*) and normal (*N*) DNA samples after bisulfite modification. PCR products in lanes M were obtained with primers for the methylated sequence (109 bp), whereas products in lanes U were obtained with primers for the unmethylated sequence (105 bp). Examples of cases in which the hypermethylation is present only in tumor DNA (*1* and *2*); one of the less abundant cases in which the hypermethylation was seen in both tumor and normal DNA (*3*); one of the cases in which the normal and tumor DNA are unmethylated (*4*).

Table 1. Comparison of clinical and pathologic variables with *Int6* expression in stage I NSCLC patients

Variable	*Int6* expression		*P*
	Low	High	
Age (mean ± SD, y)	62.9 ± 6.8	63.2 ± 6.3	NS (0.7163)
Smoking habits* (%)			
Smoker	15 (63)	38 (59)	NS (0.920)
Former smoker	8 (33)	24 (38)	
Nonsmoker	1 (4)	2 (3)	
Tumor size (%)			
T1	11 (41)	21 (28)	NS (0.334)
T2	16 (59)	53 (72)	
Histologic type (%)			
Squamous carcinoma	14 (52)	41 (55)	NS (0.740)
Adenocarcinoma	8 (30)	24 (32)	
Bronchioloalveolar carcinoma	3 (11)	7 (10)	
Large cell carcinoma	2 (7)	2 (3)	
Tumor grade (%)			
G1-2	7 (26)	21 (28)	NS (0.807)
G3	20 (74)	53 (72)	

Abbreviation: NS, not significant.
*Smoking history was available for 88 patients.

data in each case was used to normalize the results. *Int6* expression in normal tissues was extremely constant at levels similar to those found for the housekeeping genes investigated. The average levels of *Int6* RNA was found significantly higher ($P < 0.000001$) in 73% of the early-stage tumor samples compared with matching normal tissue. This, however, is not a consequence of gene amplification. The up-regulation of *Int6* RNA expression may begin during the first phases of the neoplastic growth. Although the molecular basis for Int6 up-regulation is not known, its seeming complex role in cell physiology may provide clues.

Current evidence suggests that Int6 is a multifaceted protein that interacts with components of three cellular complexes: the eIF3, the proteasome, and the constitutive photomorphogenesis 9 signalosome, to regulate their activity or to mediate signals between them. It may be that Int6 has a pivotal role in controlling protein homeostasis in physiologic and pathologic conditions, possibly regulating the translation of specific transcripts by eIF3 or the degradation of specific targets by the proteasome (15). In budding yeast, deletion mutants of the Pci8p-Int6 orthologue were found associated with decreased expression of a subset of heat shock proteins, including members of the Hsp70 family. Members of this family are known to assist other proteins in their folding, with a critical role in cell stress to prevent the appearance of misfolded or damaged molecules (4, 23). In fission yeasts, Int6 deletion mutants accumulate ubiquitinated proteins or misfolded proteins after treatment with canavanine, indicating a proteasome malfunction (9). In addition, it has been shown that Int6 binds the IFN-induced protein p56 during the course of viral infection (13, 24). Based on these and other observations, it has been suggested that Int6 may act particularly in cellular stress conditions, which cause protein misfolding during translation or ubiquitination (15). Cancer is a condition of cellular stress, in which molecular chaperons are actively involved in protein folding, translocation, and refolding of intermediates. Proteases, such as the ubiquitin-dependent proteasome, ensure that damaged and short-lived proteins are degraded efficiently (23). Based on our data, we suspect that increased *Int6* expression in lung tumors is a response to the cellular stress characterizing the neoplastic state. This could lead to increased expression of heat shock proteins by

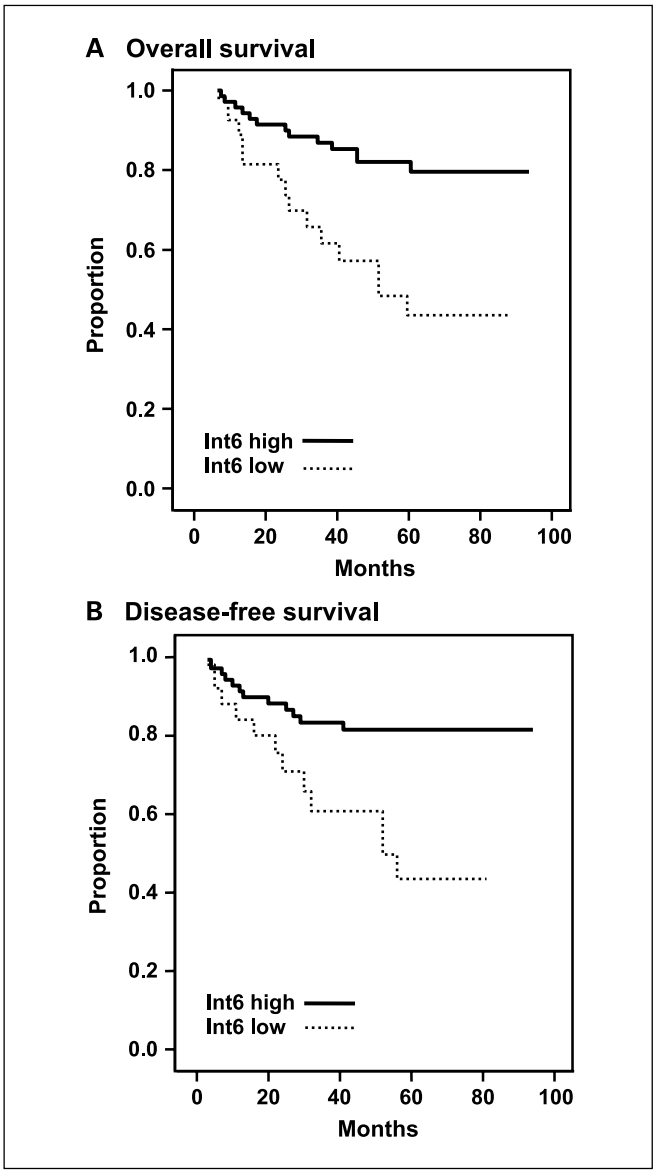

Fig. 3. Overall (*A*) and disease-free (*B*) survival curves in the 101 stage I NSCLC patients according to the *Int6* expression status in primary tumors. Curve differences are statistically significant (see text for details). *Months,* months after surgery. *Proportion,* survival proportion.

Table 2. Multivariate analysis of prognostic variables for disease-free and overall survival

Variable	β (SE)	Overall survival hazard ratio (95% confidence interval)	*P*	β (SE)	Disease-free survival hazard ratio (95% confidence interval)	*P*
Tumor size, T_1/T_2	0.92 (0.49)	2.52 (0.96-6.63)	NS (0.06)	0.83 (0.52)	2.29 (0.82-6.35)	NS (0.11)
Histologic type, SCC/non-SCC	0.47 (0.40)	1.60 (0.73-3.51)	NS (0.24)	0.49 (0.42)	1.63 (0.72-3.71)	NS (0.83)
Tumor differentiation, G1-G2/G3	0.23 (0.45)	1.25 (0.52-3.00)	NS (0.61)	0.47 (0.51)	1.61 (0.60-4.33)	NS (0.35)
Int6, reduced/increased	1.44 (0.40)	4.22 (1.91-9.28)	0.0006	1.30 (0.42)	3.67 (1.61-8.36)	0.0024

Abbreviations: β, beta coefficient; SCC, squamous cell carcinoma; NS, not significant.

activation of eIF3. In this regard, it has been reported that HSP70 can suppress the transforming properties of *p53* (25) and *c-myc* (26), two genes involved in lung tumorigenesis. On the other hand, Int6 could incrementally increase the proteosome activity to degrade misfolded or ubiquitinated proteins, such as mitotic cyclin B and securing (9, 27). In this way, Int6 could exert an important activity in neoplastic cells to maintain protein homeostasis. This is in agreement with the fact that increased Int6 RNA levels were associated with the less-aggressive tumors.

In a previous study, Northern blot analysis of a different series of 78 NSCLCs, we found a reduced expression of *Int6* in 24 (31%) tumors. Analysis of the *Int6* locus revealed that in 10 of 34 (29%) informative cases, there was LOH. However, there was no significant association between Int6 expression and LOH at the *Int6* locus. Moreover, no mutations were found in the coding region of *Int6* by single-strand conformation polymorphism assay (17). These data suggested that other mechanisms must be involved in the down-regulation of Int6. In the present study, we report evidence that a region of *Int6* located upstream and within the first exon harbours a 1,110-bp CpG island containing 55 potential methylation sites. Using a methylation-specific PCR assay, this region was found hypermethylated in 26% of cases. In the vast majority (88%) of the NSCLCs with *Int6* hypermethylation, the levels of Int6 RNA were reduced. These results indicate that in 23% of early-stage NSCLCs, *Int6* expression is decreased by epigenetic mechanisms. In only 3 of 74 tumors with high Int6 RNA levels was the gene hypermethylated. In these tumors, the levels of *Int6* RNA was moderate (i.e., a T/N ratio of <2). This would be consistent with cellular heterogeneity in the tumor with respect to hypermethylation of Int6.

Hypermethylation of *Int6* was also observed in 28% of normal lung tissues when the corresponding tumor was hypermethylated, whereas there were no cases of *Int6* hypermethylation in normal lung tissue from patients in which the tumor was not hypermethylated. Similar findings have been reported for the hypermethylation of Stratifin in breast carcinomas (28). In addition, LOH has been detected in DNA from histopathologically normal tissue adjacent to head and neck carcinomas (29) as well as breast carcinomas (30). These observations support the hypothesis that in cases where there is no atypical premalignant component of the cancer, histologically normal tissue contains genetic and epigenetic alterations that are also found in adjacent invasive tumors; representing a "field effect" in the evolution of the tumor.

Int6 RNA levels, as defined by the T/N ratio, were not significantly linked to several clinicopathologic variables including, age, smoking habits, tumor size, histologic type, and tumor grade. However, when *Int6* expression levels were compared with follow-up data, low levels of *Int6* RNA was found a significant predictor of overall and disease-free survival ($P = 0.0004$ and $P = 0.0020$, respectively). Other pathologic variables evaluated, including tumor size, histologic type, and histologic grade of the tumors were not significantly associated with prognosis. A Cox proportional hazards model that included *Int6* RNA levels and three other pathologic variables (tumor size, tumor histology, and histologic grade) still showed that low levels of *Int6* RNA had a significant independent predictive power for both overall survival ($P = 0.0006$) and disease-free survival ($P = 0.0024$).

To our knowledge, this is the first time that *Int6* mRNA levels have been accurately quantified in NSCLC samples, and that *Int6* expression has been associated with patient outcome. In our judgment, the large number of stage I patients investigated and the fact that all of the patients were treated at a single institution and received a long-term follow-up after surgery makes the survival analysis quite reliable. Our results suggest that in about one fourth of early-stage NSCLC, *Int6* expression is impaired due to methylation of transcription regulatory regions. In these cases, the tumor is more aggressive with reduced overall and disease-free survival of the patient. If our speculations are correct, induction of *Int6* overexpression could represent a possible therapeutic strategy in NSCLC patients. Additional basic and clinical studies are required to investigate the role of Int6 in cellular stress in mammalian cells, to validate the prognostic role of Int6 in cancer patients and to explore possible therapeutic approaches aimed at restoring or increasing the activity of this multifunctional protein.

Acknowledgments

We thank Dr. Barbara Vonderhaar for helpful discussions.

References

1. Marchetti A, Buttitta F, Miyazaki S, Gallahan D, Smith GH, Callahan R. Int-6, a highly conserved, widely expressed gene, is mutated by mouse mammary tumor virus in mammary preneoplasia. J Virol 1995;69:1932–8.
2. Rasmussen SB, Kordon E, Callahan R, Smith GH. Evidence for the transforming activity of a truncated Int6 gene, *in vitro*. Oncogene 2001;20:5291–301.
3. Mayeur GL, Hershey JW. Malignant transformation by the eukaryotic translation initiation factor 3 subunit p48 (eIF3e). FEBS Lett 2002;514:49–54.
4. Shalev A, Valasek L, Pise-Masison CA, et al. *Saccharomyces cerevisiae* protein Pci8p and human protein eIF3e/Int-6 interact with the eIF3 core complex by binding to cognate eIF3b subunits. J Biol Chem 2001; 276:34948–57.
5. Kim T, Hofmann K, von Arnim AG, Chamovitz DA. PCI complexes: pretty complex interactions in diverse signaling pathways. Trends Plant Sci 2001;6: 379–86.
6. Asano K, Merrick WC, Hershey JW. The translation initiation factor eIF3-p48 subunit is encoded by int-6, a site of frequent integration by the mouse mammary tumor virus genome. J Biol Chem 1997;272: 23477–80.
7. Akiyoshi Y, Clayton J, Phan L, et al. Fission yeast homolog of murine Int-6 protein, encoded by mouse mammary tumor virus integration site, is associated with the conserved core subunits of eukaryotic translation initiation factor 3. J Biol Chem 2001;276: 10056–62.
8. Bandyopadhyay A, Matsumoto T, Maitra U. Fission yeast Int6 is not essential for global translation initiation, but deletion of Int6(+) causes hypersensitivity to caffeine and affects spore formation. Mol Biol Cell 2000;11:4005–18.
9. Yen HcS, Gordon C, Chang EC. *Schizosaccharomyces pombe* Int6 and Ras homologs regulate cell division and mitotic fidelity via the proteasome. Cell 2003;112: 207–17.
10. Yahalom A, Kim TH, Winter E, Karniol B, von Arnim AG, Chamovitz DA. Arapidopsis eIF3e (Int6) associates with both eIF3c and the COP9 signalosome subunit CSN7. J Biol Chem 2001;276:334–40.
11. Hoareau Alves K, Bochard V, Rety S, Jalinot P. Association of the mammalian proto-oncoprotein Int-6 with the three protein complexes eIF3, COP9 signalosome and 26S proteasome. FEBS Lett 2002;527: 15–21.
12. Hofmann K, Bucher P. The PCI domain: a common theme in three multiprotein complexes. Trends Biochem Sci 1998;23:204–5.
13. GuoJ, Sen GC. Characterization of the interaction between the interferon-induced protein P56 and the Int6 protein encoded by a locus of insertion of the mouse mammary tumor virus. J Virol 2000;74:1892–9.
14. Watkins SJ, Norbury CJ. Cell cycle-related variation in subcellular localization of eiF3e/INT6 in human fibroblasts. Cell Prolif 2004;37:149–60.
15. Von Arnim AG, Chamovitz DA. Protein homeostasis: a degrading role for Int6/eIF3e. Curr Biol 2003;13: R323–5.
16. Miyazaki S, Imatani A, Ballard L, et al. The chromosome location of the human homolog of the mouse mammary tumor-associated gene INT6 and its status in human breast carcinomas. Genomics 1997;46:155–8.
17. Marchetti A, Buttitta F, Pellegrini S, Bertacca G, Callahan R. Reduced expression of INT-6/eIF3-p48 in human tumors. Int J Oncol 2001;18:175–9.
18. Fleming ID, Cooper JS, Henson DE, et al., editors. American Joint Committee on Cancer: cancer staging manual. 5th ed. Philadelphia (PA): Lippincott-Raven; 1997.
19. Travis TD, Colby TV, Corrin B, Shimosato Y, Brambilla, E. Histological classification of lung and pleural tumors. In: Travis WD, editor. WHO international histological classification of tumors: histological typing of lung and pleural tumors, 3rd edition. Berlin: Springer; 1999. p. 21–6.
20. Heid CA, Stevens J, Livak KJ, Williams PM. Real time quantitative PCR. Genome Res 1994;6: 986–94.
21. Herman JG, Graff JR, Myohanen S, Nelkin BD, Baylin SB. Methylation-specific PCR: a novel PCR assay for methylation status of CpG islands. Proc Natl Acad Sci USA 1996;93:9821–6.
22. Gardiner-Garden M, Frommer M. CpG islands in vertebrate genomes. J Mol Biol 1987;196:261–82.
23. Mosser DD, Morimoto RI. Molecular chaperones and the stress of oncogenesis. Oncogene 2004;23: 2907–18.
24. Guo J, Hui DJ, Merrick WC, Sen GC. A new pathway of translational regulation mediated by eukaryotic initiation factor 3. EMBO J 2000;19:6891–9.
25. Yehiely F, Oren M. The gene for the rat heat-shock cognate, hsc70, can suppress oncogene-mediated transformation. Cell Growth Differ 1992;3: 803–9.
26. Kingston RE, Baldwin AS Jr, Sharp PA. Regulation of heat shock protein 70 gene expression by c-*myc*. Nature 1984;312:280–2.
27. Yen H-cS, Chang EC. Int6. A link between the proteasome and tumorigenesis. Cell Cycle 2003;2: 81–3.
28. Umbricht CB, Evron E, Gabrielson E, Ferguson A, Marks J, Sukumar S. Hypermethylation of 14-3-3 sigma (stratifin) is an early event in breast cancer. Oncogene 2001;20:3348–53.
29. Califano J, van der Riet P, Westra W, et al. Genetic progression model for head and neck cancer: implications for field cancerization. Cancer Res 1996;56: 2488–92.
30. Deng G, Lu Y, Zlotnikov G, Thor AD, Smith HS. Loss of heterozygosity in normal tissue adjacent to breast carcinomas. Science 1996;274:2057–9.

Clinical Cancer Research

Int6 Expression Can Predict Survival in Early-Stage Non–Small Cell Lung Cancer Patients

Fiamma Buttitta, Carla Martella, Fabio Barassi, et al.

Clin Cancer Res 2005;11:3198-3204.